Intercellular Adhesion Strengthening As Studied through Simulated Stress by Organic Acid Molecules in Potato (*Solanum tuberosum* L.) Tuber Parenchyma

Ilan Shomer*,† and Lene Kaaber‡

Agricultural Research Organization, The Volcani Center, P.O. Box 6, Bet Dagan, 50250, Israel, and Norwegian Food Research Institute, MATFOSK, Osloveien, 1, N-1430, Ås, Norway

Received March 19, 2006; Revised Manuscript Received July 9, 2006

Intercellular adhesion in some parenchyma becomes strengthened in response to stress. The present study provides an approach to investigate this phenomenon (usually attributed to pectin methyl esterase and binding of Ca^{2+} and/or rhamnogalacturonan-II−borate) through reliable stress simulation by probing organic acid molecules in potato tuber parenchyma. Short-chain monocarboxylic acids induce consistent intercellular adhesion strengthening (3.8−5.3 newton) at pH ≥ 3 < pK_a, where pectin methyl esterase activity and Ca^{2+} or borate binding are limited, and vice versa at pH > pK_a with a strength of 1.4−2.0 newton as compared to 0.3−0.4 newton for the nonincubated control. Strengthening of intercellular adhesion is characterized by prominent staining of pectin and protein and immunogold labeling of pectin in the cell wall and the middle lamellar complex, particularly after boiling. Pectin confers strengthening to the primary cell wall, as reflected by: (i) prominent immunogold labeling following boiling; and (ii) puncturing macerated cells by starch gelatinization pressure after enzymatic pectin removal.

Introduction

Intercellular adhesion (ICA) in plant tissues is conferred by functional properties of the middle lamella complex (MLX). This phenomenon has been ascribed to an MLX−pectin assembly and its neutral sugars,[1,2] proteins,[3−6] phenolics,[7,8] and ions.[9,10] The ICA-strengthening phenomenon differs for various organs/species and undergoes changes during development, maturation, and ripening.[11,12] For instance, some parenchymas soften upon ripening due to loosening or liquefaction of the MLX−pectin.[13−18] In parenchymas such as potato tuber, carrot root, or bean cotyledons, ICA loosening requires incubation with exogenous pectinase.[19,20] Such parenchymas undergo MLX−pectin degradation by heat-induced β-elimination.[15,21,22] However, although pectin is known to be heat degradable, the cell wall electrical potential of boiled macerated cells of potato tuber parenchyma is ca. −70 mV and is sensitive to ions.[9,10] The cell wall charge indicates the presence of charged agents (such as protein−/pectin−COO^- groups) in the primary cell wall.

The MLX pectin was studied as a major agent in relation to intercellular adhesion. The pectin itself is biosynthesized in the Golgi,[1,23] migrates to the cell wall,[24,25] and thence into the middle lamella, being its major component. Pectins comprise 17 different monosaccharides[2] with a galacturonan core backbone 1,4-linked α-D-Gal*p*A (GA), consisting of homogalacturonan (HG), rhamnogalacturonan [→4)-α-D-GalA-(1→2)-α-l-Rha-(1→] (RG), and xylogalacturonan. At least 10−14 contiguous unesterified galacturonyl residues are required to create stable cross-linked chains, to become Ca−pectate gels.[2] The galacturonans include RG, arabinogalactan, arabinan, and galactan. The molecular nature of the galaturonan and its bonding are typical for each cell wall region.

Pectin was studied in parenchyma such as potato tuber with regards to ICA strengthening as induced by stresses such as high temperature,[26,27] anoxia, or reducing agents.[28] The ICA strengthening is a latent hardening syndrome, because it is imperceptible in viable parenchyma; however, it becomes apparent on failure to boil-soften.[27,29] Usually, ICA strengthening is attributed to Ca−pectate formed following demethoxylation by potato tuber pectin methyl esterase, which is optimally active around pH 7,[30−33] a mechanism termed here "PDCa". In the context of PDCa, immunogold labeling was used to identify both high and low methoxyl pectin (LMP and HMP, respectively) and Ca−pectate.[34] Although extracts from ICA-strengthened tissues exhibited pectin methyl esterase activity, neither the causal role of this enzyme in vivo nor the involvement of Ca−pectate in the strengthening has been demonstrated directly or consistently. In addition to Ca−pectate, borate is also cell wall covalently bound via RG-II dimers during cell growth.[35−38] Thus, borate was suggested to play a role in intercellular adhesion strengthening.[39,40] The relative content of RG-II dimers was found to be affected by both pH and other cations.

In accordance with the possible roles of PDCa and/or borate in ICA strengthening, mechanistic hypotheses require consideration of potato tuber anatomy, which is comprised of pith, parenchyma, cortex, and periderm. The periderm contains phellogen, forming inwardly phelloderm and outwardly suberized phellem cells.[41,42] The periderm differentiates to withstand environmental impact and also evidences ICA strengthening by its resistance to boiling-/enzymatic-pectin degradation. Following pathogenic/physical stress, the damaged tissue surface undergoes healing accompanied by assembly of the phenolic and aliphatic domains of suberin.[41,43−46] The interior of potato tuber tissue responds to stresses by browning, darkening, and necroses,[47,48] where cellular rupture generates superoxide radicals and polyphenol oxidase activity.[49,50] Enzymatic browning of substrates such as chlorogenic acid and tyrosine may lead to formation of melanin and complexes with cross-linked pro-

* Corresponding author. Phone: +972-3-968 3706. Fax: +972-3-960 4428. E-mail: ilans@int.gov.il.
† Agricultural Research Organization.
‡ Norwegian Food Research Institute.

10.1021/bm060256i CCC: $33.50
Published on Web 09/29/2006

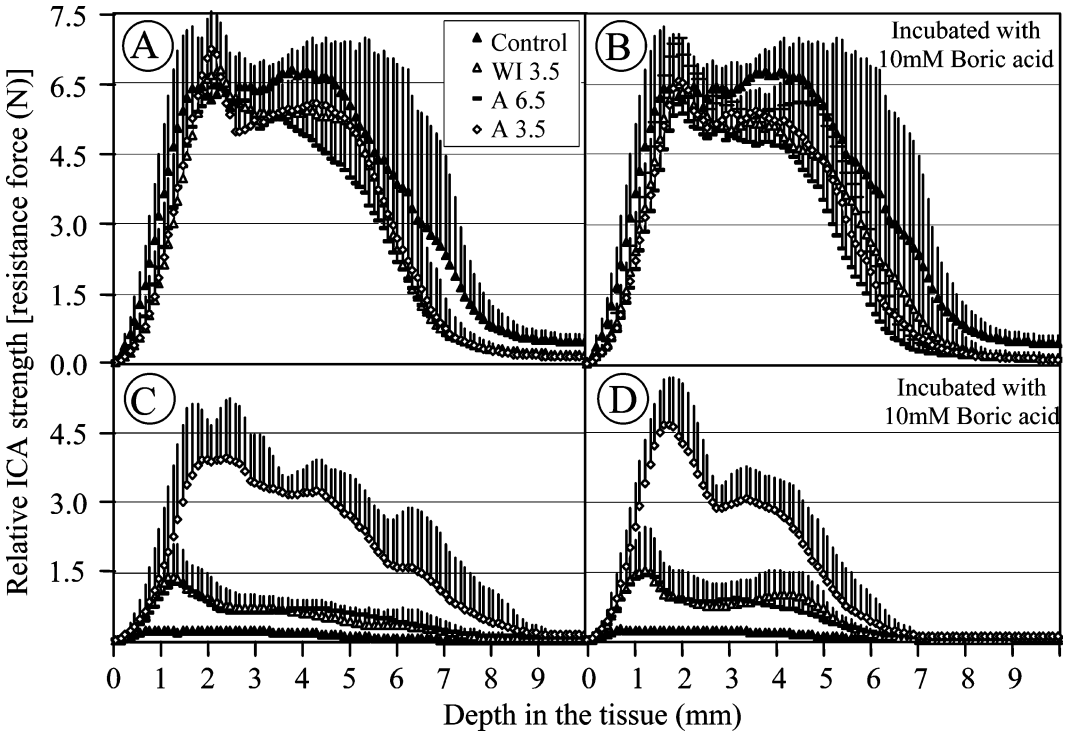

Figure 1. Relative intercellular adhesion strength (ICA) of potato tuber parenchyma [expressed as resistance force profiles (N) for penetration of 2-mm diameter cylindrical probe], following incubation with buffered acetate at pH 3.5 (A 3.5) and at pH 6.5 (A 6.5) at 65 °C for 120 min as compared to water-incubated (WI) and nonincubated tissue (control). (A) Control and incubation treatments as above; (B) is as (A) where the incubated medium included 10 mM boric acid; (C and D) are as (A) and (B), respectively, but after boiling. Bars indicate standard deviation of four repetitions and four replicates (four tubers and four slices of each).

tein.[47,50] Phenolic domains such as ferulic acid and suberin-like agents are thought to play a role in cell wall and ICA strengthening.[7,51,52]

Generally, as induced under stress, the role of PDCa and/or borate in stress-induced ICA strengthening is inconsistently documented in mature tissue, whereas assembly of polyphenols and suberin is well established in epidermal ICA-strengthened tissue of outer cell layers. Thus, it is hypothesized that (either apart from/or in accordance with PDCa and/or RG-II−borate) proteins in conjunction with phenolic, suberin-, or lignin-like domains, or some of their intermediates, precursors, and secondary metabolites, induce ICA strengthening in some parenchyma such as potato tuber.

The present study demonstrated a new idea to induce reliable and consistent ICA strengthening in response to stress, as simulated by organic acid molecules and reflected and assayed by restrained boil-softening. Stress was exerted by the combined effects of organic acids, pH's, temperatures, and buffer concentrations. ICA strengthening as reflected by boil-resistant MLX−pectin was identified by light microscopy staining, ultrastructure, and immunogold labeling. These findings are analyzed and discussed about addressing hypothesized roles of protein and phenolics in the ICA-strengthening (considering the concepts that relate the ICA-strengthening to PDCa and RG-II−borate).

Materials and Methods

Induction of Intercellular Adhesion Strengthening. Potato (*Solanum tuberosum*, L.) tubers of cvs. Sava, Desiree, and Mondial were used for this research. Medium size potato tubers were taken randomly from a 25 kg batch, hand peeled, and immersed in water at room temperature. Without delay, 2-cm thick cross slices were cut from each side of the small equator, four slices total, incubated (1:3 w/v) in aqueous medium in a beaker that was maintained in a water bath at the required temperature, and covered by aluminum foil. The liquid in the beaker was replaced with fresh medium every 20 min to maintain a constant pH. Following incubation for 60 min, the slices were rinsed twice with water, and ICA strengthening was assessed by resistibility of the tissue to be softened (due to boiling resistant of the MLX) by boiling for 20 min in a beaker with one layer of 3-mm glass beads (to prevent stickiness) and being placed on paper toweling on aluminum foil for 30 min pending texture analysis. Each slice then was cut into two halves (for texture analysis without and with boiling). Each of the treatment conditions for illustrative datasets is presented in the Results, including statistical analysis for four repetitions, each with 2−4 replicates.

Assessment of Intercellular Adhesion Strengthening by Texture Analysis. ICA strength was assessed by a texture analyzer (TA-XT2, Micro Stable Systems, Surrey, UK) by means of two parameters. (a) Profile of resistance force [newton (N)] was measured using a 2-mm diameter cylinder probe (SMS P/2). The probe was lowered at a rate of 1 mm s^{-1} through an 8-mm parenchyma slice centered on a platform with a 4-mm diameter hole in its center to permit undisturbed penetration through the tissue. (b) Maximum resistance force was measured using a 7.5-mm diameter ball probe (SMS P/0.25S). The probe was lowered at a rate of 0.3 mm s^{-1} into a 16-mm diameter tissue cylinder taken from the outer 20 mm of tuber parenchyma (after removal of 1 mm of the outermost layer). The tissue cylinder was mounted within a stainless steel ring in a radial direction. The sample was placed vertically on a platform with a central hole of 8 mm diameter enabling undisturbed penetration. The data were processed via the *Texture Expert for Windows Operating System*, Stable Micro Systems, Surrey, UK, software in Microsoft Excel.

Statistical analysis of ICA strength was performed as an expression of texture, and data were stabilized (to obtain constant variance) by transformation to log scale. The data were then analyzed by the general linear model [SAS package (Release 8.02)] including multiple comparisons test (Student−Newman−Keuls) at $\alpha = 0.05$.

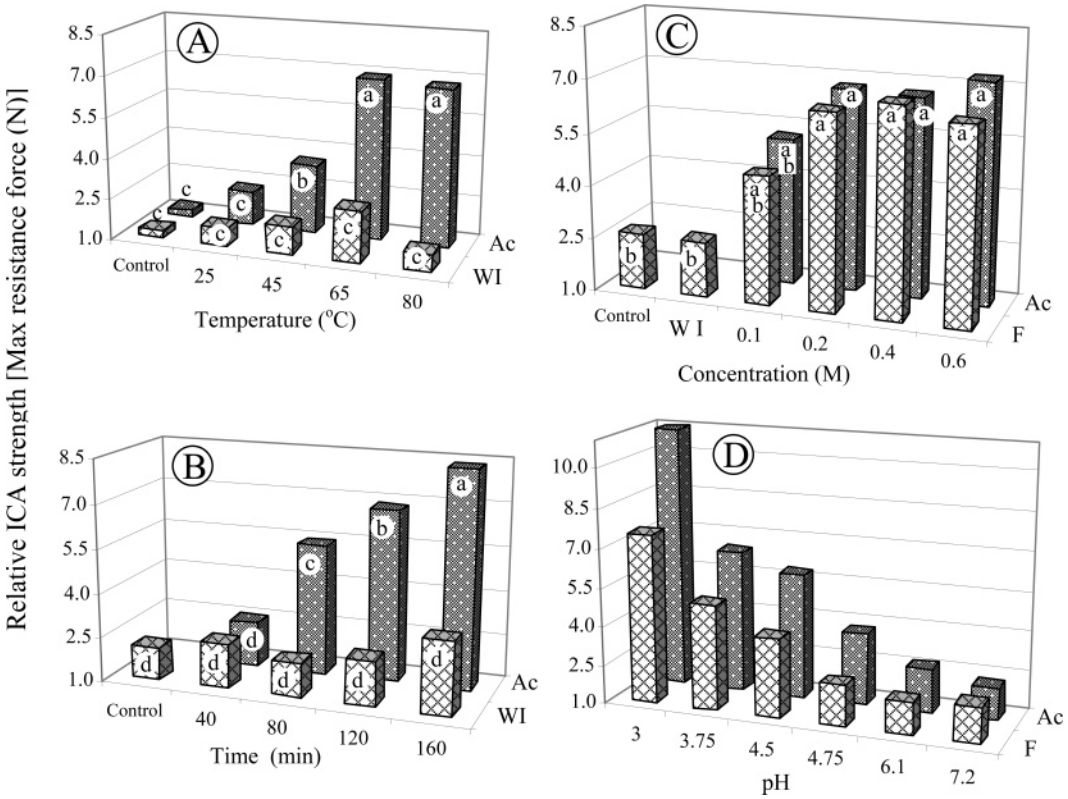

Figure 2. Relative intercellular adhesion strength [expressed by maximum resistance force (N) for penetration of 7.5-mm diameter ball probe] of potato tuber parenchyma (cv. Sava), following different incubation protocols and boiling. (A) Incubated in 0.2 M acetate buffer (Ac) at pH 3.5 or water (WI) for 60 min at various temperatures. (B) At pH 3.5 at 65 °C, for various durations in 0.2 M acetate buffer (Ac) or water (WI). (C) pH 3.5 at 65 °C in various concentrations of acetate (Ac) or formate (F) buffers. (D) 0.2 M formate (F) and acetate (Ac) buffers, at 65 °C, for 60 min. Control and WI represent nonincubated and water-incubated control, respectively. Columns with the same letter are not significantly different (Table 2).

Statistical analyses were performed for variations of ICA strengthening as an expression of texture; data were stabilized by transformation to log scale. The data then were analyzed by the general linear model [SAS package (Release 8.02)] including multiple comparisons test (Student−Newman−Keuls) at $\alpha = 0.05$.

Cell Maceration, Starch Separation, and Discerning Cell Wall Weakening. Ten grams of 1−2 mm cubes of potato tuber parenchyma was immersed in water with 1% (w/v) pectinase [Sigma P4300 (crude powder, 400−800 units/g)] and 0.001% Na-azide and shaken overnight at 37 °C, and then filtered through a strainer (Cell Dissociation Sieve−Tissue Grinder Kit, Sigma Cat. No. CD-1) of 40 mesh (Sigma Cat. No. S0770; pore size 0.42 mm), with gentle rinsing in flowing water, separating single cells. The macerated cells were suspended in distilled water in a calibrated cylinder and allowed to settle, after which the upper suspension with cell debris was removed by vacuum. This procedure was repeated until clean intact single cells were observed under the microscope. Birefringence indicated the retention of the cell wall cellulose lattice.

Starch granules were isolated by crushing 10 g of tissue cubes (~2 mm) in distilled water with a blender (Osterizer) for 20 s, incubated at 37 °C while shaking overnight with 0.1% w/w cellulase (Onozuka, Yakult Biochemicals Co.) and 0.001% Na-azide. The cellulase degraded the cell wall effectively in distilled water, allowing release of the starch grains from the cells. The suspension was poured through a sieve (Cell Dissociation Sieve−Tissue Grinder Kit, Sigma Cat. No. CD-1), using consecutively screens of 40- and 60-mesh [Sigma Cat. No. S0770 and S1020 (pore sizes 0.42 and 0.25 mm), respectively]. The separated starch granules of the filtrate were suspended in distilled water in a graduated cylinder and allowed to settle, and the upper suspension with cell debris was removed by vacuum. This procedure was repeated until microscopic examination showed clean starch grains, which were dehydrated by ethanol and then acetone, dried, and kept desiccated. Heat swelling was performed by suspending and gently shaking 100 mg of starch powder in 15 mL of distilled water in a tube at the required temperature and time. Weakening of the cell wall, judged by its puncture as a result of swelling pressure as exerted by intracellular gelatinizing starch, was detected by light microscope on separated cells. To retain undisturbed spatial structure for observation by a light microscope, a 70 μL suspension (of either starch grains or macerated cells) was mixed homogeneously with 0.5 mL of 2% agar solution at 50 °C, and a drop of the mixture was poured and flattened upon a glass slide within a 2 × 2 cm square of silica grease of 1 mm walls that was placed on a hot plate at 50 °C. A cover glass was placed on the silica grease frame with the suspension, and then it was cooled to ~18 °C and sealed with nail enamel.

Light Microscopy, Electron Microscopy, and Immunogold Labeling. Sections (2 × 2 × 4 mm) of outer parenchyma, adjacent to the cortex, were prepared for either ultrastructural observations or immunogold labeling.[53,54] The immunogold labeling was of epitopes from 0 to 40−50% pectin methoxylation by monoclonal antibody (mAb) JIM5 and of 15−80% methoxylation by mAb JIM7.[55] Accordingly, in the present study, because pectin epitopes of ~15−80% methoxylation were immunogold labeled by mAb JIM7 and undetectable by mAb JIM5, which is bound to epitopes of less than 40−50% methoxylation,[55] they are termed here methoxylated pectin and LMP, respectively. For ultrastructural study, the tissue sections were prepared and observed according to Shomer[22] and Shomer et al.[56]

Immunogold labeling was done according to Hall and Hawes[57] and Lurie et al.[54] with some modification. Tissue sections were fixed overnight in 3.5% (w/v) glutaraldehyde and 2% paraformaldehyde in 0.1 M pH 7.0 cacodylate buffer, rinsed in cacodylate buffer, and dehydrated gradually by 30%, 50%, 70%, and 96% ethanol−water solutions for 15 min each, followed by pure ethanol for 1 h. Sections then were infiltrated gradually by LR-White and hardened in embedding moulds (covered with polycarbonate strip in contact with the resin surface to prevent oxidation) in an oven at 60 °C for 24 h. Ultrathin

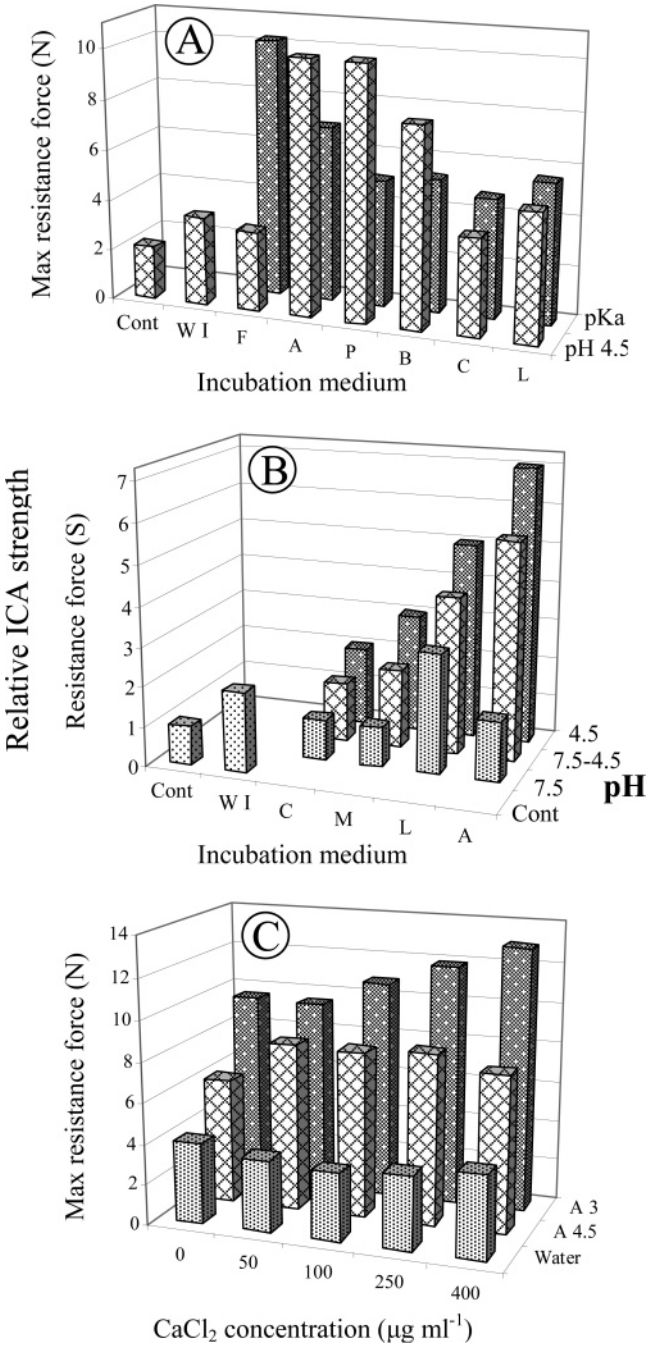

Figure 3. Relative intercellular adhesion force [as maximum resistance force (N) sensory grade (S) for penetration of 7.5-mm diameter ball probe] of potato tuber parenchyma (cv. Sava), incubated in 0.2 M buffer at 65 °C and boiled. (A) Buffers at pK_a and pH 4.5. (B) pH regimes as follows: 7.5, pH 7.5 for 2 h; 7.5−4.5, pH 7.5 for 1 h followed by pH 4.5 for 1 h; 4.5, pH 4.5 for 2 h. (C) Incubation in water or acetate at pH 3.5 or 4.5 with various $CaCl_2$ concentration. Incubation buffers: A, acetate; B, butyrate; C, citrate; F, formate; L, lactate; M, malate; P, propionate; WI, water incubated.

sections upon nickel grids were placed for 15 min on a drop of blocking buffer [1% (w/v) bovine serum albumin (BSA), 0.02% Na-azide, and 0.05% Tween 20 in tris-buffered saline (TBS: 10 mM Tris-HCl, pH 7.4, and 10 mM MaCl)], facing the solution. The grid was then incubated for 1 h in 1:100−200 diluted primary rat mAb of either LMP (JIM5) or methoxylated pectin epitope (JIM7) in the blocking buffer. The grid was rinsed successively by 5 drops of TBS, incubated for 1 h in a 20 μL drop of secondary goat anti-rat mAb-gold (IgG), rinsed in TBS as above, and post-fixed for 3 min in 1% glutaraldehyde in TBS, rinsed in distilled water, and stained by uranyl-acetate and lead-citrate. Immunogold labeling was performed also after chemical demethoxylation by immersion of a grid with ultrathin sections in 1 mL of 0.1 M Na_2CO_3 for 20 min, and then washed thoroughly with distilled water. Transmission electron microscope (JEOL-100CX) observations were made at 80 kV.

For light microscopy, transverse sections of 2 μm thickness were prepared from the LR-White embedded tissue, loaded on a glass slide, stained with ruthenium red for pectin identification or by Coomassie brilliant blue R 250 [Merck, Germany (0.25 g in 100 mL of water, which includes 45.4 mL of MeOH and 9.4 mL of concentrated acetic acid)] for protein. Starch granules, macerated cells, and tissue sections were observed by a light microscope (Axioskop, Zeizz, Germany; with Nikon camera DMX1200F).

Table 1. Relative Intercellular Adhesion Strength [(Mean ± SD) Expressed as Maximum Resistance Force (N) for Penetration of 2 mm Diameter Cylindrical Probe] of 6−8-mm Thick Tuber Parenchyma Slices Incubated in 0.2 M Buffer Acetate at 65 °C for 120 min[a]

I (cvs. Compare)				
	Desirée		Mondial	
incubation medium	control	boiled	control	boiled
buffer acetate, pH 3.5	5.7 ± 0.2b	3.8 ± 0.5a	4.8 ± 0.5a	4.3 ± 0.1a
buffer acetate, pH 6.5	5.3 ± 0.1b	1.4 ± 0.4b	4.6 ± 0.2a	1.0 ± 0.5c
water	4.7 ± 0.2c	1.4 ± 0.7b	4.6 ± 0.7a	2.0 ± 0.5b
fresh nontreated	6.6 ± 0.3a	0.4 ± 0.1c	4.9 ± 0.3a	0.4 ± 0.1c
II (Borate Effect, cv. Desirée)				
	control		with 10 mM boric acid	
incubation medium	nonboiled	boiled	nonboiled	boiled
buffer acetate, pH 3.5	6.9 ± 0.7	5.3 ± 0.8	6.7 ± 0.5	4.3 ± 0.7
buffer acetate, pH 6.5	6.7 ± 0.5	1.4 ± 0.3	6.5 ± 0.5	1.5 ± 0.2
water	6.9 ± 0.6	1.5 ± 0.7	6.6 ± 0.5	1.8 ± 0.8
fresh nontreated	7.3 ± 0.8	0.3 ± 0.1	7.3 ± 0.8	0.3 ± 0.1

[a] Samples of cv. Desirée I and II were from different batches of tubers. Values designated by the same letter are not significantly different ($p < 0.01$). The correlation coefficient between maximum force and force−profile area (Figure 1) is 0.98.

Table 2. Properties of Organic Acid Buffers Used To Induce ICA Strengthening (as Resistance Force Presented in Figure 3A,B) and the Significance of Its Differences among Treatments at pH = pK_a and at pH 4.5

buffer	acid formula	MW	MV[a]	log K_{ow}[b]	pK_a value
formate	HCOOH	46.02	37.72	−0.54	3.75a[c]
acetate	CH_3COOH	60.05	57.23	−0.17	4.78b
propionate	CH_3CH_2COOH	74.08	74.60	0.33	4.87b
butyrate	$CH_3CH_2CH_2COOH$	88.10	91.99	0.79	4.82b
lactate	$CH_3CHOHCOOH$	90.08	72.12	−0.72	3.83cb
malate	$HOCHCOOHCH_2$-COOH	134.09	83.34	−1.26	3.04; 5.05
citrate	$CH_2(COOH)\cdot$ $COH(COOH)\cdot$ $CH_2(COOH)$	192.12	115.39	−1.72	3.14; 4.77; 6.39cb

[a] Molar volume ($m^3\ mol^{-1}$). [b] Octanol/water partition coefficient. [c] Same letter indicates an insignificant difference among either pK_a or pH 4.5 values ($\alpha = 0.05$).

Results

Intercellular Adhesion Strength. Stress response ICA strengthening in parenchyma is efficiently and consistently assessed when simulated by organic acids and is detectable by a restrained degree of boil-softening. This is demonstrated when acetate buffer at pH 3.5 (<pK_a) induced significant ICA strengthening in potato (*Solanum tuberosum* L.) tuber parenchyma, as verified in two cultivars Desirée and Mondial.

The latent hardening is illustrated by the textural profile of the potato parenchyma, where all of the treatments resulted in

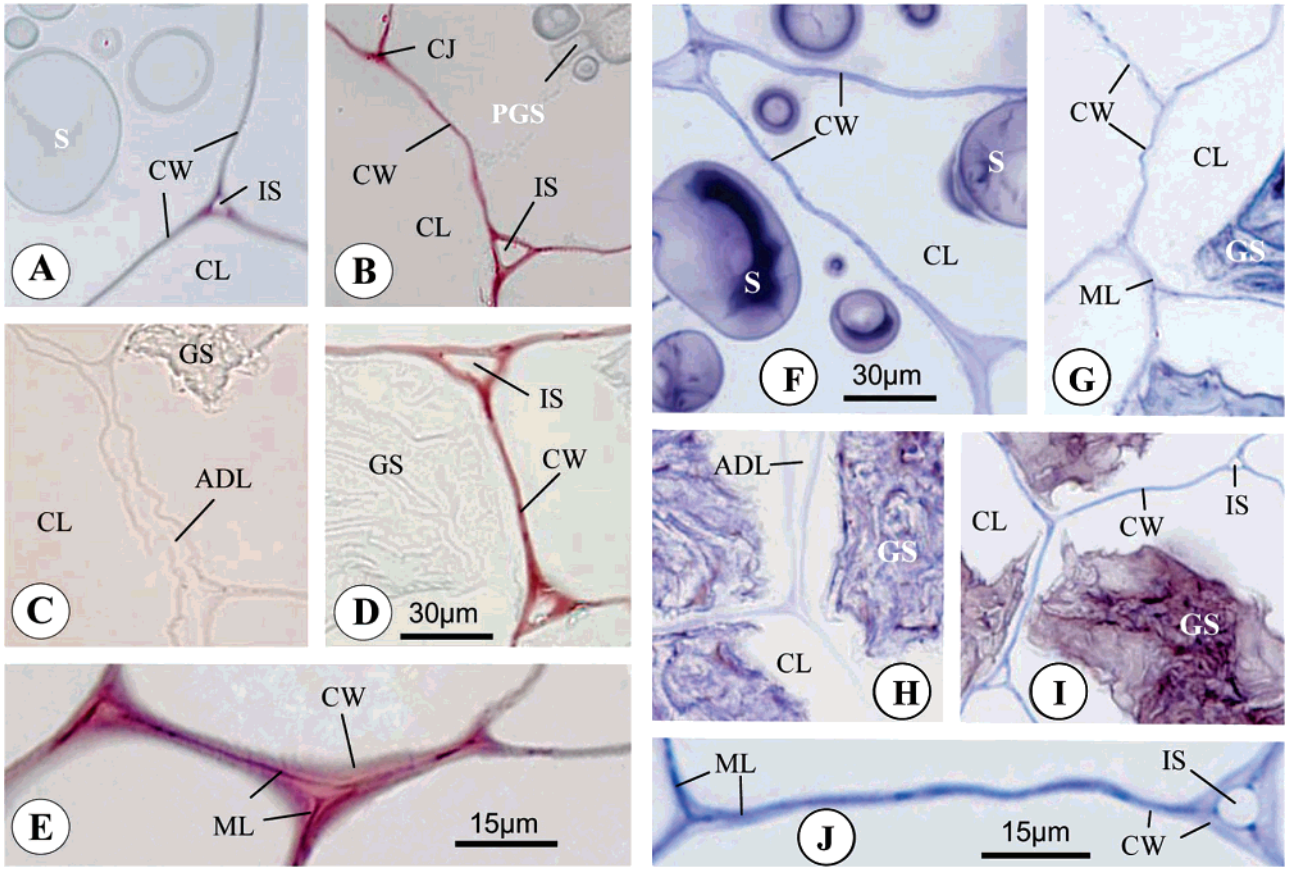

Figure 4. Transverse sections of potato tuber parenchyma stained with ruthenium red for pectin (A−E) and with Coomassie brilliant blue for protein (F−J). (A,F) Control untreated. (B,G) Incubated in 0.2 M acetate at pH 3.5 for 2 h at 65 °C. (C,D,H,I) are as (A), (B), (F), and (G) but after boiling, respectively (A−D, F−I, bar = 15 μm). (E,J) are as (D) and (I), respectively, at higher magnification. ADL, area of degraded middle lamella; CJ, cell junction; CL, cell lumen; CW, cell wall; GS; heat gelatinized starch; ML, middle lamella; IS, intercellular space; S, starch.

similar strengths with overlapping standard deviations (Figure 1A and B). The hardened tissue becomes evident and significantly differs from the controls only after boiling degradation of the middle lamella (Figure 1C and D).

Tissue incubated at pH 3.5 and boiled had significantly ($p < 0.01$) higher ICA-strengthening profiles than those induced at pH 6.5 and water, and these were significantly different from nonincubated tissue. In each of these treatments, organic acid molecules caused prominent intercellular adhesion strengthening upon other effects where no marked effect was found due to the presence of borate (Table 1).

The induced ICA strengthening by acetate buffer at pH 4.5 ($<pK_a$) depended on the incubation regime, whereas the maximum resistance force increased with temperature up to 80 °C, and time and concentration up to 0.2 M (Figure 2A−C). Both formate and acetate buffers induced significant ICA strengthening that increased with decreasing pH from 7.5 to 3.5 (Figure 2D). Various acid buffers induced ICA-strengthening levels with significant differences between some of them and/or among pH 4.5, 7.5 and pH = pK_a (Figure 3A and B, Table 2).

At pH = pK_a, formate buffer induced the highest intercellular adhesion resistance, and at pH 4.5 it was acetate and propionate. The ability to induce ICA strengthening was compared under several pH regimes (Figure 3B), showing that resistance of potato tuber parenchyma varied according to citrate < malate < lactate < acetate. This trend is correlated with the lipophilicity of the octanol/water partition coefficient of the acid molecules, where at pH = pK_a, it correlated inversely with the acid molar volume (Figure 3, Table 2).

Significant ($p < 0.001$) differences were obtained among incubation regimes, which were considered as nine treatments (including controls) in each experimental set (Figure 2A−C). As illustrated for short chain-/linear-/monocarboxylic acids, the linear term of ICA strengthening due to pH change was significant ($p < 0.001$), also after including it in the model ($p < 0.02$), where acetate induced a significantly ($p < 0.004$) higher effect than did formate (Figure 2D, Table 2).

ICA that was induced under pH 4.5 (Figure 3A) behaved obviously according to the pH level being either above (>) or below (<) the pK_a of each specific acid [for formate ($>^{cb}$), acetate ($<^{a}$), propionate ($<^{a}$), butyrate ($<^{a}$), lactate ($>^{b}$), malate ($>^{b}$), and citrate ($>^{cb}$)], where the same uppercase letter indicates insignificant differences ($\alpha = 0.05$).

Statistically, about the same differences were obtained by both texture analysis and sensory grade [Figure 3B, see Materials and Methods], with correlation coefficient >0.9. Both RG-II−borate complex (Figure 1) and Ca^{2+} (Figure 3C) did not cause marked ICA strengthening, where significant differences were obtained among water, acetate at pH 4.5, and acetate at pH 3.5 incubations.

Pectin and Protein Staining. Light microscopy showed that the cell wall of the control and acetate-induced tissue at pH 3.5 was stained distinctly for pectin (Figure 4A,B) and protein (Figure 4F,G). Staining for pectin and protein was absent in boiling degraded MLX (Figure 4C,H). Both pectin (Figure 4D,E) and protein (Figure 4I,J) are prominent in the middle lamellar zone of strengthened ICA tissue, particularly after boiling.

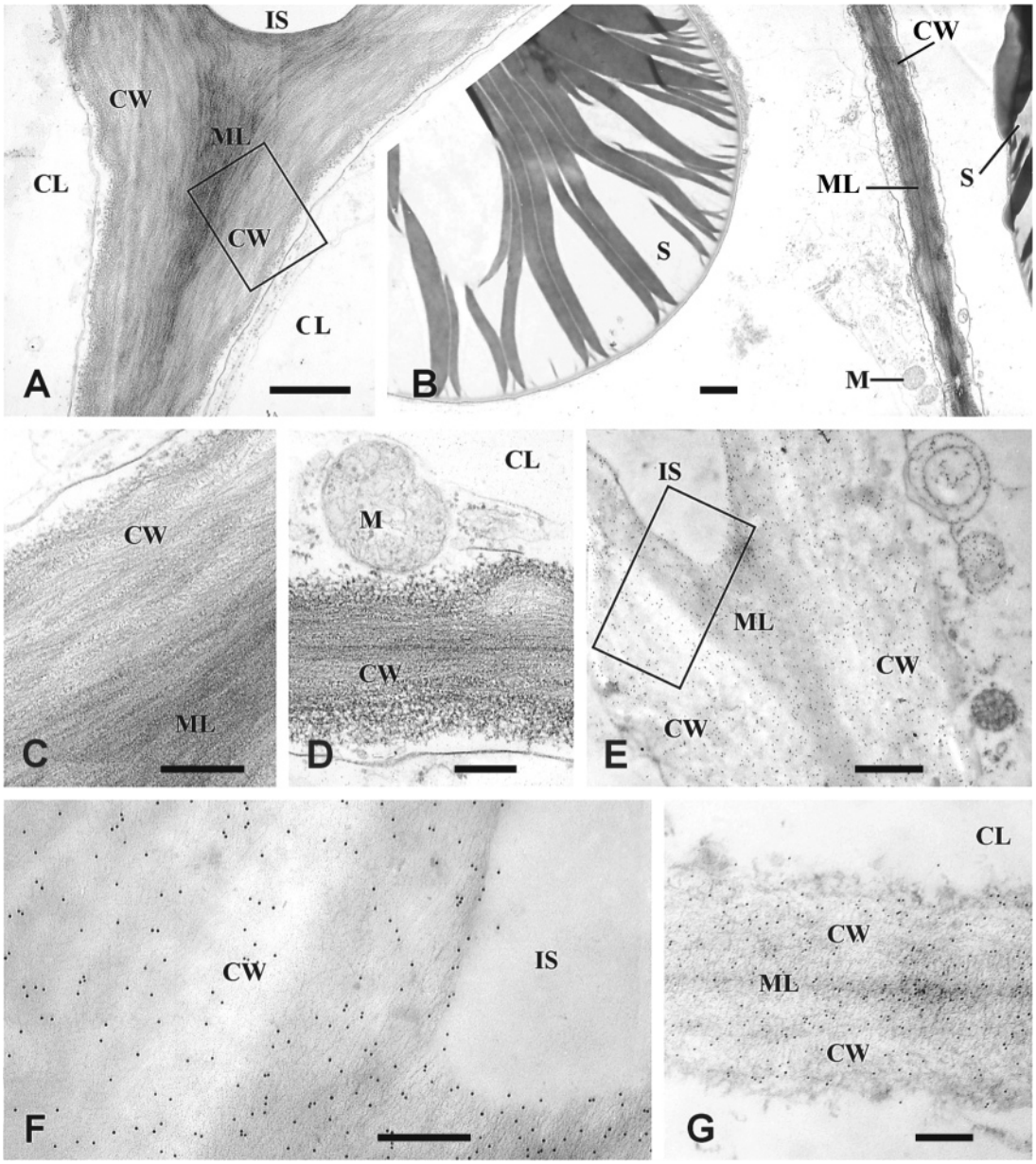

Figure 5. Transverse ultrasections of potato tuber parenchyma. (A,C) Cell wall patterns and adjacent intercellular space. (B,D) Cellular adhesion planes. (E) and its inset (F), and (G), are the same as (A−D) but labeled with mAb JIM7. CL, cell lumen; CW, cell wall; IS, intercellular space; M, mitochondria; ML, middle lamella; S, starch. (A,B,E) bar = 1 μm; (C,D,F,G) bar = 0.3 μm.

Cell Wall Structure and Pectin Localization. The primary cell wall and the lamella are relatively thick beside the cell junction and intercellular space (Figure 5A,C) but are thin along cell adhesion planes (Figure 5B,D). Labeling of a pectin epitope by mAb JIM7 is seen in the primary cell wall, the middle lamella, and the intercellular space rims (Figure 5E,F) as well as along cell adhesion planes (Figure 5G).

As a result of boiling, the middle lamella was degraded and cell wall lattice was sparser (Figure 6A and B). The MLX degradation is well observable where adjacent cells detached from each other (Figure 6C, D, and F). However, it is worth noting that, despite that the middle lamella underwent boiling degradation, the pectin embedding the cellulose lattice was found to be retained as it is distinctly shown by immunogold labeling of methoxylated pectin epitope (Figure 6A−F).

In ICA-strengthened tissue induced by acetate at pH 3.5 < pK_a (Figure 1), the cell wall lattice was relatively dense with a prominently electron dense middle lamella at cell junctions (Figure 7A) and along cell adhesion planes (Figure 7B). As found in viable (Figure 5) and boiled tissue (Figure 6), also in ICA-strengthened tissue, methoxylated pectin epitope was identified in cell junctions, intercellular space rims, and along cell adhesion planes either before (Figure 7C and D) or after boiling (Figure 7E−G). However, the LMP epitope was undetectable.

To demonstrate that potato tuber parenchyma could be labeled for LMP epitope, chemical demethoxylation of ultrathin sections by Na_2CO_3 was followed by immunogold labeling, using mAb JIM5. Immunogold labeling of the LMP epitope by mAb JIM5 was clearly observed in both viable (Figure 8A and B) and boiled tissue (Figure 8C and D). After boiling, LMP epitope was found at intercellular space rims (Figure 8C and D); the epitope appeared sparse in an adjacent region (Figure 8D) and absent along cell adhesion planes, from which the middle lamella was degraded by boiling (Figure 8E and F). In ICA-strengthened tissue, immunogold labeling of LMP epitope by mAb JIM5 was observed adjacent to intercellular spaces (Figure 8G) as well

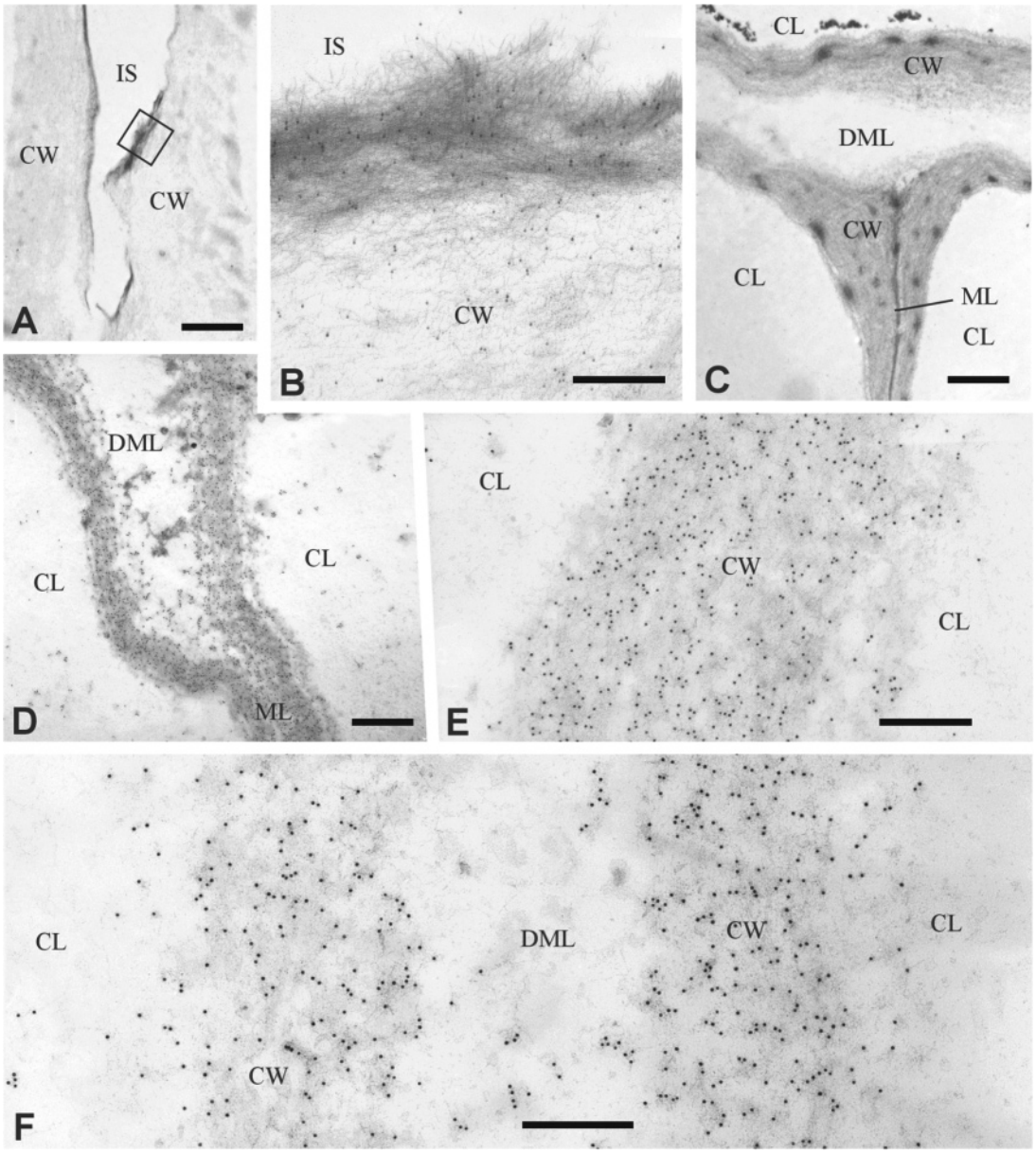

Figure 6. As Figure 5 but after boiling and immunogold labeling for methoxylated pectin by mAb JIM7. (A and its inset B) Cell wall adjacent to intercellular space. (C) A cell junction region where middle lamella residues are observed beside boil-degraded middle lamella. (D) Cell adhesion plane where states of attached and detached cell walls seen beside each other. (E,F) Higher magnification of sites where adjacent cell walls are attached and detached, respectively. CL, cell lumen; CW, cell wall; DML, area of degraded middle lamella; IS, intercellular space; ML, middle lamella. (A,C) bar = 2 μm; (B,E,F) bar = 0.3 μm; (D) bar = 1 μm.

as along cell adhesion planes both before (Figure 8H) and after (Figure 8I) boiling.

For comparison, immunogold labeling of methoxylated pectin epitope was examined following chemical demethoxylation by Na_2CO_3. Obvious immunogold labeling of methoxylated pectin epitope is seen in viable (Figure 8J), boiled (Figure 8K and L), and ICA-strengthened tissue, of which middle lamella is retained (Figure 8M).

Cell Structure under Pressure of Endogenous Gelatinized Starch. The MLX−pectin is assembled continuously with the pectin embedding the cellulose lattice (Figures 5E−G and 7C−F). Thus, evaluation of ICA strength also requires assessment of the strength of the primary cell wall, which can be studied in single intact cells (Figure 9), in the absence of tissue support.

The impact of pectin may be tested due to whether pectin degradation weakens cell resistance against internal pressure exerted by swollen gelatinized starch.

Polarized light and dark field conditions revealed various stages of heat starch gelatinization at 64 °C (Figure 9C), yet the cells seemed intact. The starch swelling potential to exert pressure is illustrated in Figure 10A−D, which shows various stages of swelling and birefringence in either separated or intracellular granules. The gelatinization process is initiated in the hilum and progressed toward the periphery of the granules (Figure 10B−D). Within the transition temperature range, the various granules differ in heat-gelatinization sensitivity (Figure 10B), and variations also occurred among cells (Figures 9C and 10D).

Single gelatinized granules appear large, sometimes almost as big as the cells themselves (Figure 10D), whereas granule swelling inside the cells is restricted (Figures 9C and 10D) by the cell wall. Weakening of the cell wall as a result of enzymatic pectin maceration is deduced from observation of punctures caused by swollen starch pressure, when temperature was

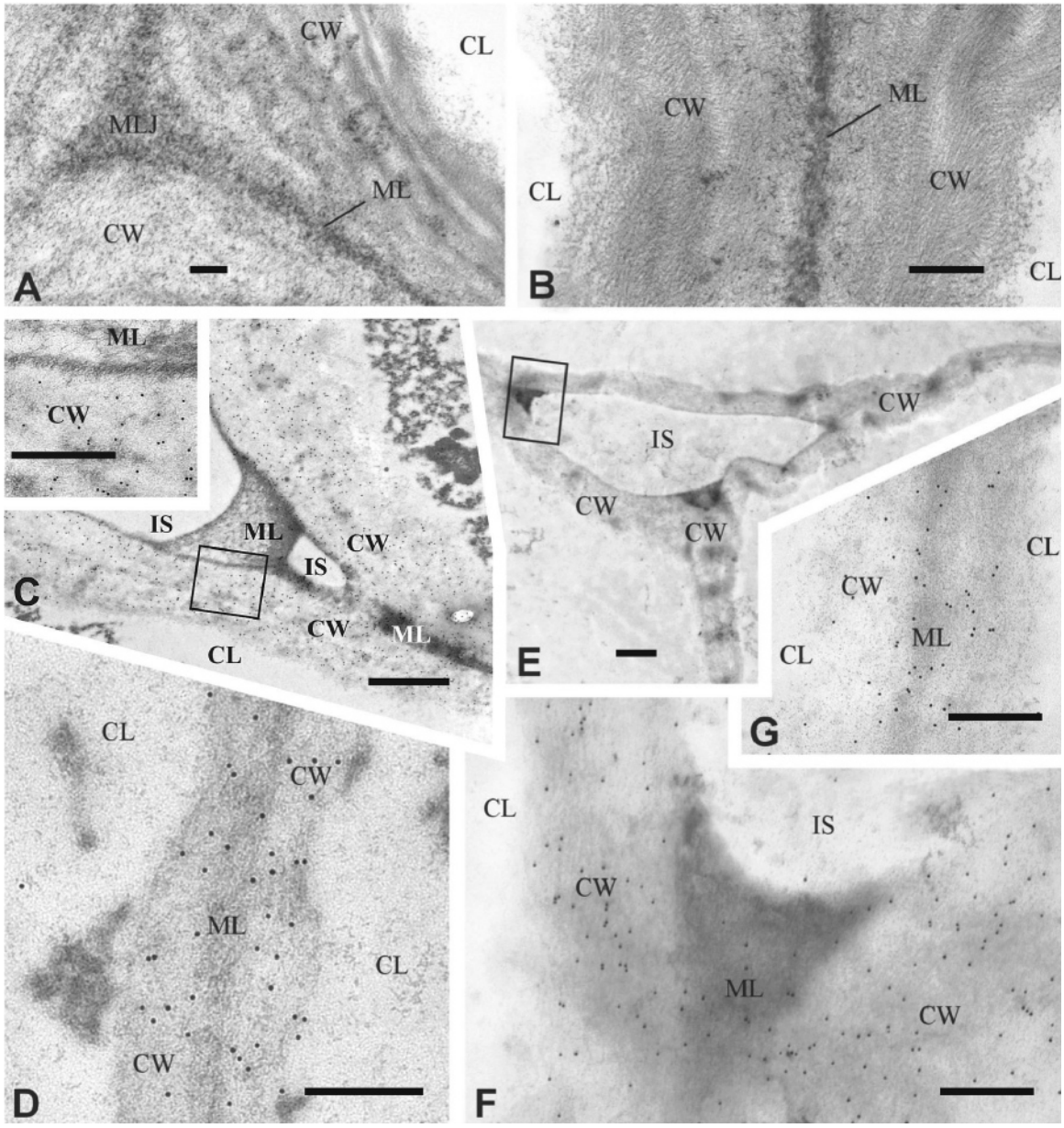

Figure 7. As in Figure 5, but of PTP that was induced for ICA strengthening by acetate at pH 3.5, 65 °C for 60 min. (A,B) Regions of cell junction and adhesion plane, respectively, where the middle lamella zone is prominent and electron dense. (C) and its inset (D) are as (A,B) but immunogold labeled for methoxylated pectin by mAb JIM7. (E) and its inset (F), and (G) are as (C,D) but following boiling. CL, cell lumen; CW, cell wall; IS, intercellular space; ML, middle lamella; MLJ, middle lamella junction. (C,E) bar = 1 μm; (A,B and insets of C,D,F,G) bar = 0.3 μm.

increased to 68 °C for 10 min (Figure 10E). Starch extrusion increased after heating for an additional 5 min at 70 °C (Figure 10F). The clear cell wall birefringence indicates well retaining of the cellulose lattice in the primary cell wall.

Discussion

Study of the ICA strengthening, in response to stress of mature parenchyma, necessitates consistent and reliable assembly of the agents involved so that they may be identifiable. In the present study, short chain-/linear-/monocarboxylic acids are shown to be an efficient tool to study the mechanism involved in simulated stress-induced ICA strengthening. The known ICA factors Ca−pectate and/or RG-II borate complex have been referred to here in relation to simulated stress-induced strengthening.

The involvement of pectin methyl esterase and Ca−pectate is inconsistently documented in relation to ICA strengthening.[26,28−31] For example, stress of 60 °C induced hardening, although pectin methyl esterase is more active at 25−50 °C.[25,31] Moreover, strengthening is induced at 75 °C if pH < pK_a (Figure 2), but PDCa is limited,[29] while at pH > pK_a, particularly above pH 6 the strengthening is limited (Figures 1−3), although PDCa is optimal.

In the pH range examined (Figures 1−4), the trend of Ca^{2+} binding increases with pH similarly to the trend of boron binding [$B(OH)_3^0 + H_2O \leftrightarrows B(OH)_4^- + H^+$], correlating with the relative content of RG-II dimers.[36] However, short-chain monocarboxylic acids induce minor ICA strengthening at pH > pK_a, although the covalently bound $B(OH)_4^-$ is relatively high and vice versa at pH < pK_a, where borate binding is extremely low.[59,60] Moreover, near pH = pK_a, minor pH changes produced significant strengthening alteration (Figures 1−4) where RG-II dimer content is similar.[38] Nevertheless, borate (Figure 1) and calcium had little effect on ICA strength, particularly at pH >

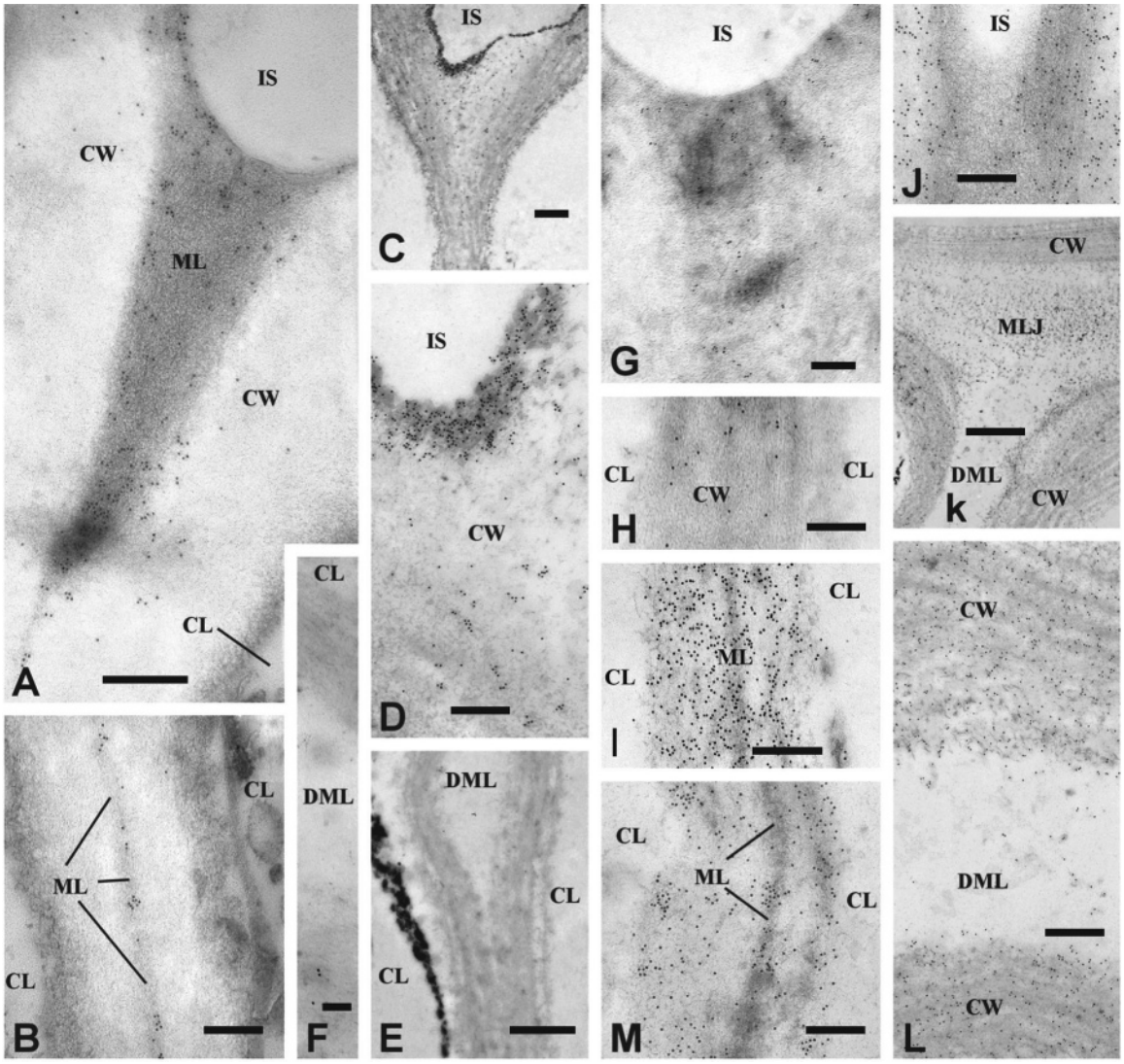

Figure 8. Ultrathin sections that underwent chemical demethoxylation by Na_2CO_3 and are immunogold labeled. (A,B) A region adjacent to intercellular spaces and adhesion plane, respectively, immunogold labeled for LMP by JIM5. (C,E) and their insets (D,F) are as in (A,B), but following boiling. (G,H) are as (D,F), respectively, after induction for ICA strengthening by acetate buffer at pH 3.5, 65 °C for 60 min. (I,J) Viable tissue after chemical demethoxylation immunogold labeled for methoxylated pectin by JIM7 at the adhesion plane and adjacent intercellular space, respectively. (K,L) Labeling of boiled chemical demethoxylated tissue by JIM7, at the cell junction and adhesion plane, respectively. (M,L) After induction for ICA strengthening by acetate buffer at pH 3.5, 65 °C for 60 min. CL, cell lumen; CW, cell wall; DML, area of degraded middle lamella; IS, intercellular space; ML, middle lamella; MLJ, middle lamella junction. (C,E,K) bar = 1 μm; (A,B,D,G,J,L) bar = 0.3 μm; (F) bar = 80 nm; (H,I,M) bar = 0.2 μm.

pK_a (Figure 3), where PDCa is optimal. Thus, the role of RG-II−borate in stress response ICA strengthening deserves further elucidation.

Organic acids induction of strengthened MLX−pectin directly or indirectly is dependent on an association between organic acid molecules/anions and a defined tissue site(s). Because relatively minor pH changes result in large ICA alterations near pH = pK_a where strengthening is induced at pH < pK_a, it appears that the strengthening is induced by the lipophilic acid molecules, rather than by the pH per se. The lipophilic nature of the organic acid molecules as related to ICA strengthening is in agreement with the octanol/water partition coefficient (Table 2). This finding suggests that ICA strengthening is induced when acid molecules associate with lipophilic cell compartment(s). In addition, the inverse correlation between ICA strengthening and acid molar volume at pH = pK_a (Table 2) suggests that the acid molecules associate with relevant sites due to their solubility/infusibility in the tissue. Hence, ICA strengthening in water (Figure 1) is attributable to H_2CO_3 (pH = pK_a is 6.35). In this context, a possible involvement of Ca−organic acid complex in ICA strengthening is dubious, because strengthening is induced at pH < pK_a, where calcium binding is restrained, and vice versa at pH > pK_a. Moreover, acids such as citric and lactic induce relatively moderate strengthening. On the other hand, experiments in Shomer's laboratory (manuscript in preparation) showed that monocarboxylic acids of longer chain length (such as decanoic) induce ICA strengthening at any pH from 3 to 7.5.

That immunogold labeling is obtained only by mAb JIM 7 [recognizing 15−80% methoxylation[53] but not JIM5 (Figures 6−8)] suggests that both the primary cell wall and the MLX include pectin of 40/50−80% methoxylation. Thus, the weighted net negative charge of ~ −70 mV in the cell wall and its apparent sensitivity to exchangeable ions[9,10] may indicate the presence of protein with methoxylated pectin (Figure 4). In this context, the occurrence of demethoxylated pectin, as detected by silver-enhanced gold,[34,61] may be unspecific. However, the identification of either methoxylated or LMP pectin by conju-

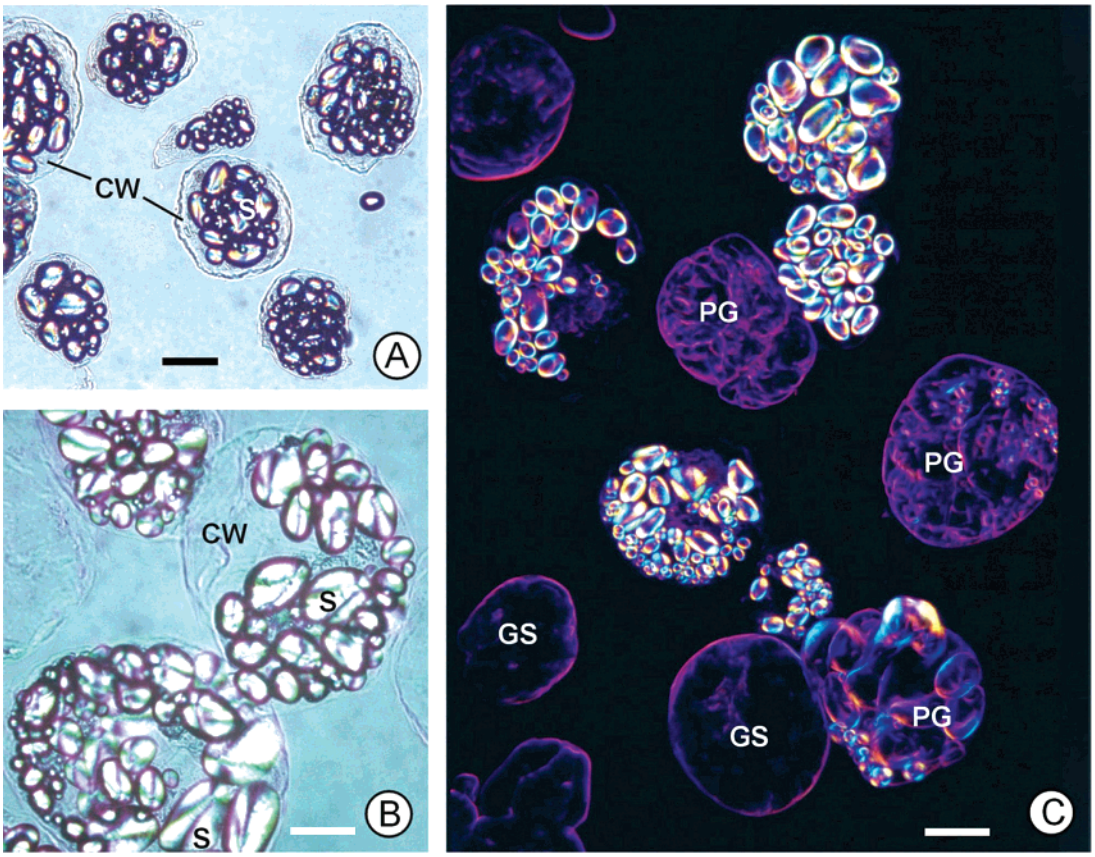

Figure 9. Light microscopy of cells after enzymatic maceration. (A,B) Viewed by polarized light. (C) Cells heated at 64 °C for 10 min, viewed under polarized light and dark field. CW, cell wall; GS, gelatinized starch; PG, partially gelatinized starch; S, starch. (A,C) bar = 100 μm; (B) bar = 20 μm.

gated gold (Figures 6−8) is highly specific. Moreover, the low demethoxylation is verifiable in chemically demethoxylated cell wall, where labeling by mAb JIM5 was distinctly lower than by JIM7 (Figure 8).

Structurally and functionally, MLX−pectin is continuous with the primary cell wall pectin. Thus, ICA strength is connected to the strength of the pectin embedding the cellulose lattice, as reflected by its boil resistance (Figure 6).[9,22] Following enzymatic pectin removal,[15,17,20] the weakened cell wall is punctured by starch gelatinization pressure (Figure 10). Noticeably, despite enzymatic pectin removal, the cellulose lattice is retained, as discerned by the cell wall birefringence (Figure 10) and ultrastructure[62] (not shown here for macerated cells of potato tuber parenchyma) and by the cells' integrity even after heating to 64 °C for 10 min and partial starch gelatinization (Figure 9). Moreover, the ultrastructure (not shown) and the birefringence were retained even after cell puncturing (Figure 10). Therefore, here ICA strengthening [Figures 1−3, assessed by boiling resistance] occurs in the range of 40/50−80% methoxylated MLX−pectin (Figures 5−8).

The ordinary strength of pectin varies between the middle lamella and the cellulose lattice, as reflected by its boil resistance (Figures 6 and 7) and/or chemical demethoxylation (Figure 8). These findings are plausible with the relatively moderate cross-linking of MLX−pectin/Ca−pectate, whereas the pectin embedding the cellulose lattice is interwoven through hairy/branched agents (covalently bound RG-II−borate, RG-I, XGA, AG-I/II, A, hemicellulose),[2] proteins,[6] phenolics,[7,52] and ions.[9,10]

Thus, ICA strengthening is presumably conferred by stronger MLX than ordinarily exists with Ca−pectate and RG-II−borate complex as: (a) Pectin is labeled by mAb JIM7 and not by mAb JIM5 in both control and ICA-strengthened tissue (Figures 5−7), without increase in demethoxylation.[32] (b) Prominent pectin/protein staining (Figure 4) in cell wall of boiled ICA-strengthened tissue (Figures 1−3) following incubation in conditions in which PDCa and RG-II−borate binding is known to be limited, and vice versa.

The relatively thick zones of prominent electron dense patterns in ICA-strengthened tissue (Figure 7A,B), detected around the thin middle lamella (Figure 5B,D), are suggested to be composed of proteins (Figure 5E,J) and suberin-like phenolics.[52] These patterns appear after stress, as simulated by organic acid molecules (Figure 7). Boiling intensified the pectin/protein staining (Figure 4D,E,I, and J) and compacted the ultrastructure of the electron dense patterns (Figure 7E−G) in the middle lamellar zone; indicating heat coagulation[63] of pectin-associated proteins in the middle lamellar zone. Stress response ICA strengthening could be attributed to association of the MLX−pectin with protein or phenolics. For instance, ICA-strengthened tissue has amorphous electron dense MLX (Figures 7 and 8), typical to that of lignified[7,64] or sclerified parenchyma.[54] Lignin-/suberin-like phenolics may be involved in ICA strengthening by binding with MLX−pectin.[52,63−65] The present findings led us to induce in vitro ICA strengthening, allowing consistent assembly of the related agents. Then, the induced in vitro ICA-strengthening was found to be associated exclusively with both cell wall bound protein (prominently identified in the middle lamellar zone)[68] and suberin-like phenolics.[52] Furthermore, protein staining in conjunction with the MLX-pectin in ICA-strengthened tissue [(Figures 4E, 7C−F) which appeared as a

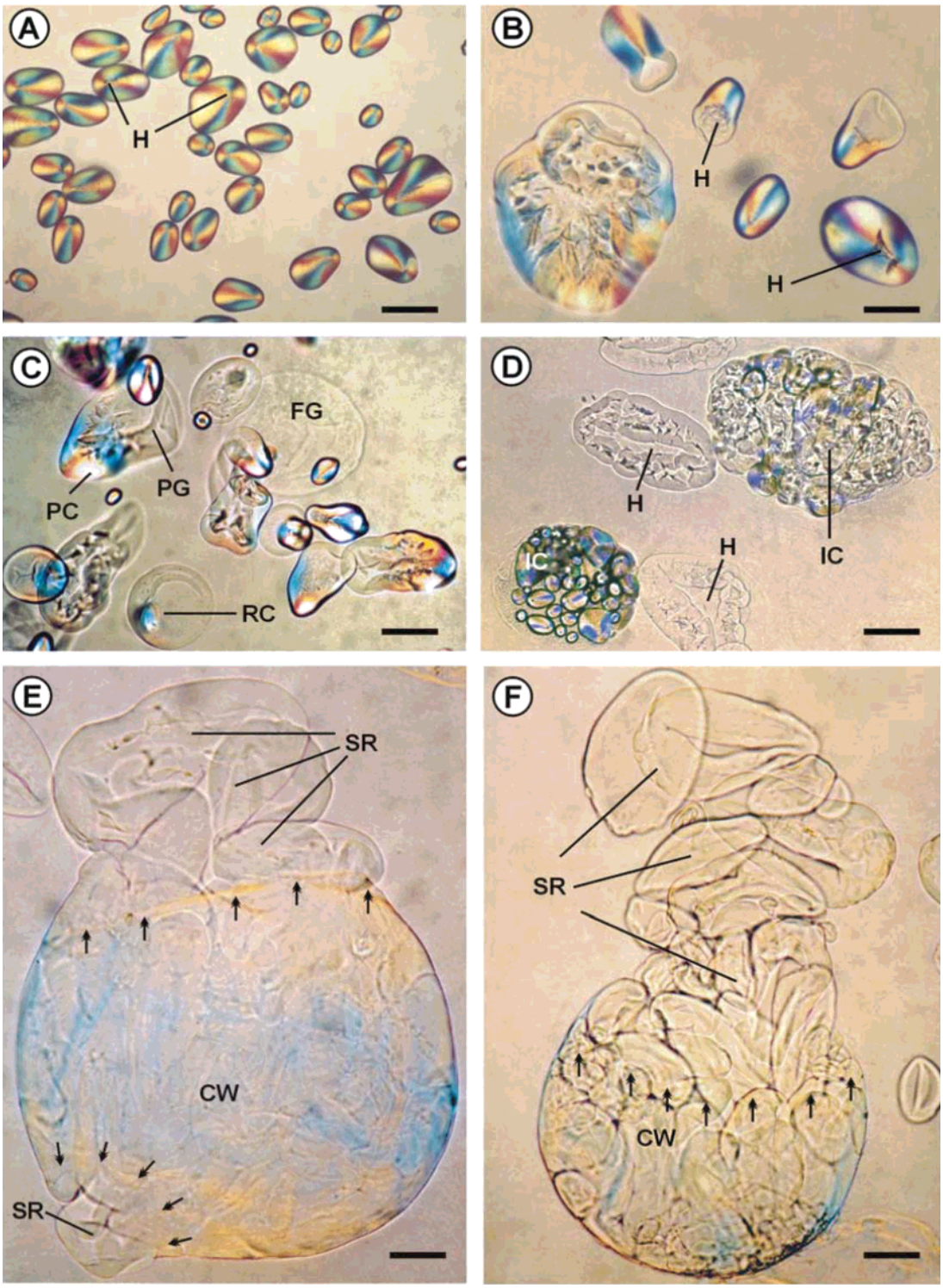

Figure 10. Starch viewed under polarized light and its structural alterations upon heating at 64 °C. (A−C) Unheated, heated for 5 and 10 min, respectively. (D) is as (C) where single starch grains are seen beside intact cells. (E) Cells heated at 68 °C for 10 min, showing punctured cell wall caused by swollen starch pressure. (F) is as (E), but cell heated for 15 min at 70 °C, where the extruded starch is seen to have progressed. CW, cell wall; FG, fully gelatinized starch; H, hilum; IC, intracellular starch; PG, partially gelatinized starch; RC, remnant of crystalline pattern; S, starch; SR, starch released from punctured site. Arrows point to the punctured cell wall rim. (A−D) bar = 20 μm; (E,F) bar = 40 μm.

thickened electron dense zone particularly after boiling (Figures 4J, 7B)], is also associated with suberin-like agents.[52] Consequently, these results suggest that the middle lamella of ICA-strengthened tissue comprises a complex of pectin, protein, and suberin-like phenolics.

In conclusion, organic acid molecules induce ICA strengthening in the presence of >40−50% methoxylated pectin under conditions in which PDCa is known to be inhibited. Conversely, following incubation in the presence of organic acid anions under conditions that facilitate the occurrence of PCDa and/or RG-II-borate complex at pH > pK_a, the MLX structure exhibits mild strengthening (if at all), where the middle lamella is loosened upon boiling. Our further study[52] demonstrated the use of simulated stress response by organic acids for the molecular characterization of intercellular adhesion strengthening.

Acknowledgment. The research was supported by the US-Israel Binational Agricultural Research and Development Fund, Award No. I.S.-3368-02 from BARD, and by the Nordic Industrial Foundation − Project No. 98110. We appreciate and thank the critical scientific and editorial discussions with Dr. Victor Gaba (ARO, Israel), Dr. Ruth Stark (City University of New York), Dr. Mikhail Borisover, and Dr. Rami Keren (ARO, Israel). Thanks are due to Dr. Paul J. Knox (University of Leeds, UK) for his kind advice and for supplying the antibodies. Thanks are due to Tatiana Yefremov and Liana Jashi, ARO, Israel, and to Tone Bergersen, MATFORSK, Norway, for their excellent technical assistance. This is Contribution No. 429/05 from the ARO, The Volcani Center, Bet Dagan, Israel.

Note Added after ASAP Publication. This article was released ASAP on September 29, 2006. In the Discussion section, paragraph 10, sentence 2 has been revised. The correct version was posted on October 19, 2006.

References and Notes

(1) Lord, E. M.; Mollet, J.-C. *Proc. Natl. Acad. Sci. U.S.A.* **2002**, *99*, 15843−15845.
(2) Vincken, J.-P.; Schols, H. A.; Oomen, R. J. F. J.; McCann, M. C.; Ulvskov, P.; Voragen, A. G. F.; Visser, R. G. F. *Plant Physiol.* **2003**, *132*, 1781−1789.
(3) Anderson, C. M.; Wagner, T. A.; Perret, M.; He, Z. H.; He, D.; Kohorn, B. D. *Plant Mol. Biol.* **2001**, *47*, 197−206.
(4) Cosgrove, D. J. *Plant Physiol. Biochem.* **2000**, *38*, 109−124.
(5) Robertson, D.; Mitchell, G. P.; Gilroy, J. S.; Gerrish, C.; Bolwell, G. P.; Slabas, A. R. *J. Biol. Chem.* **1997**, *272*, 15841−15848.
(6) Showalter, A. M. *Cell. Mol. Life Sci.* **2001**, *58*, 1361−1362.
(7) Modafar, C. E.; Tantaoui, A.; Boustani, E. E. *J. Phytopathol.* **2000**, *148*, 405−411.
(8) Wallace, G.; Fry, S. C. *Int. Rev. Cytol.* **1994**, *151*, 229−267.
(9) Shomer, I.; Frenkel, H.; Polinger, C. *Carbohydr. Polym.* **1990**, *16*, 199−210.
(10) Shomer, I.; Novacky, A.; Pike, S.; Yermiyahu, U.; Kinraide, T. B. *Plant Physiol.* **2003**, *133*, 411−422.
(11) Jarvis, M. C.; Briggs, S. P. H.; Knox, J. P. *Plant, Cell Environ.* **2003**, *26*, 977−989.
(12) Knox, J. P. *Plant J.* **1992**, *2*, 137−141.
(13) Cosgrove, D. J. *Plant Physiol.* **2001**, *125*, 131−134.
(14) Fischer, R. L.; Bennet, A. B. *Annu. Rev. Plant Physiol. Plant Mol. Biol.* **1991**, *42*, 675−703.
(15) Martin-Rodriguez, M. C.; Orchard, J.; Seymour, G. B. *J. Exp. Bot.* **2002**, *53*, 2115−2119.
(16) Orfila, C.; Seymour, G. B.; Willats, W. G. T.; Huxham, I. M.; Jarvis, M. C.; Dover, C. J.; Thompson, A. J.; Knox, J. P. *Plant Physiol.* **2001**, *126*, 210−221.
(17) Scavetta, R. D.; Herron, S. R.; Hotchkiss, A. T.; Kita, N.; Keen, N. T.; Benen, J. A. E.; Kester, H. C. M.; Visser, J.; Jurnak, F. *Plant Cell* **1999**, *11*, 1081−1092.
(18) White, P. J. *J. Exp. Bot.* **2002**, *53*, 1995−2000.
(19) Shomer, I.; Levy, D. *Potato Res.* **1988**, *31*, 321−334.
(20) van den Broek, L. A. M.; den Aantrekker, E. D.; Voragen, A. G. J.; Beldman, G.; Vincken, J.-P. *J. Sci. Food Agric.* **1997**, *75*, 167−172.
(21) Ng, A.; Waldron, K. W. *J. Sci. Food Agric.* **1997**, *73*, 503−512.
(22) Shomer, I. *Carbohydr. Polym.* **1995**, *26*, 47−54.
(23) Sterling, J. D.; Quigley, H. F.; Orellana, A.; Mohnen, D. *Plant Physiol.* **2001**, *127*, 360−371.
(24) Kohorn, B. D.; Kobayashi, M.; Johansen, S.; Riese, J.; Huang, L.-F.; Koch, K.; Fu, S.; Dotson, A.; Byers, N. *Plant J.* **2006**, *46*, 307−316.
(25) Anderson, M. C.; Wagner, A. T.; Perret, M.; He, Z.-H.; He, D.; Kohorn, D. B. *Plant Mol. Biol.* **2001**, *47*, 197−206.
(26) Stolle-Smits, T.; Beekhuizen, J. G.; Recourt, K.; Voragen, A. G. J.; van Dijk, C. *J. Agric. Food Chem.* **2000**, *48*, 5269−5277.
(27) van Dijk, C.; Fischer, M.; Beekhuizen, J.-G.; Boeriu, C.; Stolle-Smits, T. *J. Agric. Food Chem.* **2002**, *50*, 5098−5106.
(28) Sapers, G. M.; Miller, R. L. *J. Food Sci.* **1995**, *60*, 762−766.
(29) Shomer, I.; Paster, N.; Lindner, R.; Vasiliver, R. *Food Struct.* **1990**, *9*, 139−149.
(30) MacKinnon, I. M.; Jardine, W. G.; O'Kennedy, N.; Renard, C. M. G. C.; Jarvis, M. C. *J. Agric. Food Chem.* **2002**, *50*, 342−346.
(31) McMillan, G. P.; Pérombelon, M. C. M. *Physiol. Mol. Plant Pathol.* **1995**, *46*, 413−427.
(32) Micheli, F. *Plant Sci.* **2001**, *6*, 414−419.
(33) Stolle-Smits, T.; Beekhuizen, J. G.; Kok, M. T. C.; Pijnenburg, M.; Recourt, K.; Derksen, J.; Voragen, A. G. J. *Plant Physiol.* **1999**, *121*, 363−372.
(34) Bush, M. S.; McCann, M. C. *Physiol. Plant.* **1999**, *107*, 201−213.
(35) Blevins, D. G.; Lukaszewski, K. M. *Annu. Rev. Plant Physiol. Plant Mol. Biol.* **1998**, *49*, 481−500.
(36) Ishii, T.; Matsunaga, T.; Hayashi, N. *Plant Physiol.* **2001**, *126*, 1698−1705.
(37) Loomis, W. D.; Durst, R. W. *BioFactors* **1992**, *3*, 229−239.
(38) O'Neill, M. A.; Eberhard, S.; Albersheim, P.; Darvill, A. G. *Science* **2001**, *294*, 846−849.
(39) Ryden, P.; Sugimoto-Shirasu, K.; Smith, A. C.; Findlay, K.; Reiter, W.-D.; McCann, M. C. *Plant Physiol.* **2003**, *132*, 1033−1040.
(40) Singh, S. K.; Eland, C.; Harholt, J.; Scheller, H. V.; Marchant, A. *Plant J.* **2005**, *43*, 384−397.
(41) Fabbri, A. A.; Fanelli, C.; Reverberi, M.; Ricelli, A.; Camera, E.; Urbanelli, S.; Rossini, A.; Picardo, M.; Altamura, M. M. *J. Exp. Bot.* **2000**, *51*, 1267−1275.
(42) Yan, B.; Stark, R. E. *Macromolecules* **1998**, *31*, 2600−2605.
(43) Graça, J.; Pereira, H. *J. Agric. Food Chem.* **2000**, *48*, 5476−5483.
(44) Moire, L.; Schmutz, A.; Buchala, A.; Yan, B.; Stark, R. E.; Ryser, U. *Plant Physiol.* **1999**, *119*, 1137−1146.
(45) Parr, A. J.; Ng, A.; Waldron, K. W. *J. Agric. Food Chem.* **1997**, *45*, 2468−2471.
(46) Stark, R. E.; Sohn, W.; Pacchiano, R. A., Jr.; Al-Bashir, M.; Garbow, J. R. *Plant Physiol.* **1994**, *104*, 527−533.
(47) Corsini, D. L.; Pavek, J. J.; Dean, B. *Am. Potato J.* **1992**, *69*, 423−435.
(48) Lee, G. S.; Sterrett, S. B.; Henninger, M. R. *Am. Potato J.* **1992**, *69*, 353−362.
(49) Johnson, S. M.; Doherty, S. J.; Croy, R. R. D. *Plant Physiol.* **2003**, *131*, 1440−1449.
(50) Stevens, L. H.; Davelaar, E. *Phytochemistry* **1996**, *42*, 941−947.
(51) Waldron, K. W.; Smith, A. C.; Parr, A. J.; Ng, A.; Parker, M. L. *Trends Food Sci. Technol.* **1997**, *8*, 213−221.
(52) Yu, B.; Vengadesan, G.; Wang, H.; Jashi, L.; Yefremov, T.; Tian, S.; Gaba, V.; Shomer, I.; Stark, R. E. *Biomacromolecules* **2006**, *7*, 937−944.
(53) Jones, L.; Seymour, G. B.; Knox, J. P. *Plant Physiol.* **1997**, *113*, 1405−1412.
(54) Lurie, S.; Zhou, H.-W.; Lers, A.; Sonego, L.; Alexandrov, S.; Shomer, I. *Physiol. Plant.* **2003**, *119*, 287−294.
(55) Willats, W. G. T.; Limberg, G.; Buchholt, H. C.; van Alebeek, G.-J.; Benen, J.; Christensen, T. M. I. E.; Visser, J.; Voragen, A.; Mikkelsen, J. D.; Knox, J. P. *Carbohydr. Res.* **2000**, *327*, 309−320.
(56) Shomer, I.; Chalutz, E.; Vasiliver, R.; Lomaniec, E.; Berman, M. *Can. J. Bot.* **1989**, *67*, 625−632.
(57) Hall, J. L.; Hawes, C. *Electron Microscopy of Plant Cells*; Academic Press Ltd.: London, UK, 1991.
(58) Sapers, G. M.; Cook, P. H.; Heidel, A. E.; Martin, S. T.; Miller, R. L. *J. Food Sci.* **1997**, *62*, 797−803.
(59) Keren, R.; Bingham, F. T. *Adv. Soil Sci.* **1985**, *1*, 229−276.
(60) Keren, R.; Grossl, P. R.; Sparks, D. L. *Soil Sci. Soc. Am. J.* **1994**, *58*, 1116−1122.
(61) Parker, C. C.; Parker, M. L.; Smith, A. C.; Waldron, K. W. *J. Agric. Food Chem.* **2001**, *49*, 4364−4371.
(62) Shomer, I.; Lindner, P.; Vasiliver, R. *J. Food Sci.* **1984**, *49*, 628−633.
(63) Shomer, I.; Lindner, P.; Ben Gra, I.; Vasiliver, R. *J. Sci. Food Agri.* **1982**, *33*, 565−575.
(64) Ruel, K.; Montiel, M.-D.; Goujon, T.; Jouanin, L.; Burlat, V.; Joseleau, J.-P. *Plant Biol.* **2001**, *4*, 2−8.
(65) Montiel, R. K.; Goujon, M.-D.; Jouanin, T. L.; Burlat, V.; Joseleau, J.-P. *Plant Biol.* **2002**, *4*, 2−8.
(66) Ruel, K.; Chabannes, M.; Boudet, A.-M.; Legrand, M.; Joseleau, J.-P. *Phytochemistry* **2001a**, *57*, 875−882.
(67) Wakabayashi, K.; Hoson, T.; Kamisaka, S. *Plant Physiol.* **1997**, *113*, 967−973.
(68) Vengadesan, G.; Yu, B.; Jashi, L.; Yefremov, T.; Borisover, M.; Stark, R. E.; Gaba, V.; Shomer, I. *Proc. XXIII Int. Carbohydrate Sym.* Whistler, British Columbia Canada 2006, p 291 (abstract).

BM060256I